Research & Reviews: Journal of Material Sciences
DOI: 10.4172/2321-6212.1000167

e-ISSN: 2321-6212
p-ISSN: 2347-2278

Optoelectronic Studies of Commercially and Lab Prepared Cadmium sulfide Chalcogenide

Arvind Kumar Verma*, Pramesh Chandra, Anchal Srivastava and Shukla RK

Department of Physics, University of Lucknow, Lucknow, India

Research Article

Received: 03/05/2017
Accepted: 18/05/2017
Published: 25/05/2017

***For Correspondence**

Arvind Kumar Verma, Department of Physics, University of Lucknow, Lucknow – 226007, India, Tel: 0522 2740449.

Email: verma.arvind82phd@gmail.com

Keywords: CdS powder, XRD, SEM, UV-Visible spectroscopy, Photoluminescence, FTIR

ABSTRACT

Cadmium Sulfide (CdS) chalcogenide has been prepared by co-precipitation method. Both cubic and hexagonal phases existed in the commercially obtained CdS (S1) whereas the lab prepared samples using ethanol (S2) and distilled water (S3) existed homogeneously in the cubic phase only. Average crystallite size as determined by Debye-Scherrer formula for samples S1, S2 and S3 are 20.9, 3.5 and 4.9 nm respectively. SEM images of all samples show that the surface morphologies are in the form of assemblies of nanoparticles. Absorption spectra show a peak at 538 nm for the sample S1, at 482 nm for S2 and at 516 nm for S3. Optical size as calculated by Brus equation for S1, S2, and S3 are 4.47, 4.00, and 10.96 nm respectively. Absorption coefficient of the sample decreases continuously from visible region to near ultraviolet region while absorption constant of the sample increases up to the visible region as wavelength increases. PL spectra indicate effective photoemission property in the visible region. FTIR spectra show a peak at 610 cm-1 for prepared samples S2 and S3 which is attributed to CdS formation.

INTRODUCTION

Cadmium sulfide (CdS) is one of the most important II-VI inorganic semiconductors members of the metal chalcogenide family with a direct bandgap (2.42 eV) at room temperature. It exists as two different polymorphs, hexagonal (wurtzite) form, or cubic (zincblende) form [1]. Generally; the Stable structure of cadmium sulfide at room temperature is zinc-blende, namely the cubic metastable phase whereas hexagonal crystalline phase is the thermodynamically stable phase over 300°C.The majority of the inorganic cadmium sulfide semiconductors are good candidates for electron acceptors. There are several methods to obtain CdS nanoparticles like gas phase reaction, solvothermal method, chemical bath deposition, microwave-assisted solution precipitation, and much more. These methods required high temperature with the use of toxic and highly sensitive compounds for different phase structures because different phases show different lattice vibration as well as nonlinear optical coefficients. Phase transformation processes from cubic to hexagonal phase require high temperature or high pressure. Therefore, it is of great significance to using effective co-precipitation method at low cost, fast with well controlled size and shape of semiconductor nanostructures of the cadmium sulfide by exploring novel approaches related to optical studies at room temperatures with easy preparation technique are highly attractive for desired applications in future for general purpose [2-4]. Photoactive colloidal luminescent semiconductor nanocrystals referred to as “quantum dots” or “QDs” are promising for utilizing the high-efficiency photovoltaic devices at a low cost by adjustable band gap with unique size tuning, high extinction coefficient and good photostability for sensitized solar cells. CdS QDs are more attractive due to broader utilization of the solar spectrum in the visible region with strong optical absorption in the 400 to 550 nm wavelength range.

The increase in the band gap with the decrease in the size of the particles is the most identified aspect of quantum confinement in CdS semiconductors [5,6]. Due to increase in the band gap of the CdS nanoparticles, it is widely used in optoelectronics, photonics, photovoltaic and photocatalysis. QDs are used as a window material for heterojunction solar cells to avoid the recombination of photo-generated carriers which consequently improves the efficiency of the solar cells. In optoelectronics, cadmium sulfide QDs

e-ISSN: 2321-6212
p-ISSN: 2347-2278

are used for making photocells, light emitting diode (LED), lasers, nonlinear optics, heterogeneous photocatalysis, high-density magnetic information storage and address decoders. In photonics, CdS is employed to make nanocrystals, sensors, optical filters, and all optical switches. CdS are also used as a pigment in paints and in engineered plastic for good thermal stability. These properties are the result of high surface-to-volume ratio present in CdS nanoparticles.

Various methods have been developed to synthesize cadmium sulfide in nanophase with different morphologies and structures like nanocrystals, nanorods, nanowhiskers, nanowires, nanobelts, nanotubes etc. Large-scale synthesis of semiconductor nanoparticles such as solid powder is critically important not only for the study of their physical properties but also for their industrial applications in the areas of catalysis, photocatalysis, and microelectronics [7-10].

Many fundamental properties of cadmium sulfide have been expressed as a function of size and shape, controlling these aspects of semiconductor nanocrystallites would provide opportunities for tailoring properties of materials and offer possibilities for observing interesting and useful physical phenomena. Development of synthetic strategies for CdS nanocrystals of various shapes is still very significant to the field of materials science. The influence of various reaction parameters and solvents on the morphology of CdS nanostructures have been studied extensively by various researchers [11].

In the present work, the effect of commercially obtained sample (S1) and lab prepared; samples S2 (ethanol), distilled water sample (S3) on the optical properties of Cadmium sulfide (CdS) has been studied.

EXPERIMENTAL DETAILS

In this experiment, commercially available cadmium sulfide powder procured from CDH Laboratory Reagents (maximum limits of impurities – water-soluble matter: 2%, chloride: 0.02%, nitrate: 0.002%, iron: 0.03%) was used and named as sample S1. The other two samples of CdS were prepared using ethanol and distilled water as a solvent. 2.665 g cadmium acetate was dissolved in 50 ml ethanol in a volumetric flask to make a 0.2 M ethanolic solution. Similarly, 0.781 g sodium sulfide was dissolved in ethanol to make a 0.2 M ethanolic solution. Both the solutions were kept separately for 1 hour each at room temperature before mixing them. The solution so obtained was kept under constant magnetic stirring for 1 h at 40°C for obtaining homogeneity. Ammonium hydroxide was also added to maintain a pH value of 7 at this temperature. The pH value was confirmed using pH indicator strips. The resulting yellow precipitate was separated from the solution by filtration and washed many times with ethanol as well as distilled water respectively.

Finally, the precipitate was dried in hot air oven at 60°C for 4 h and the powder so obtained was named as sample S2. The Same process was followed for the precipitation of CdS powder with distilled water as a solvent. This time, a precipitate had to be dried at 100°C for 4 h. The higher temperature was required for this sample to obtain a proper dry condition. This powder was named as sample S3. Finally, all the three samples viz. S1 (commercially obtained), S2 (prepared in ethanol), and S3 (prepared in distilled water) were ground using mortar and pestle to obtain fine CdS powder for characterization.

CHARACTERIZATION OF CDS POWDER SAMPLES

X-ray diffraction (XRD), Scanning Electron Microscopy (SEM), UV-visible absorption spectroscopy, Photoluminescence (PL) spectroscopy, and Fourier Transform Infrared (FTIR) spectroscopy carried out the characterization of the three different CdS powder samples. Crystal structures of the CdS samples were characterized by X-ray diffraction (XRD) using Regaku ultima-IV, employing CuK_{α} radiation (wavelength 1.5404 Å) in the 2θ range from 10° to 70° with a scan speed of 2°/sec under the similar conditions. Surface morphology of the samples was observed by Scanning Electron Microscope using model LEO-430 from Cambridge, England. The optical absorption spectra were recorded using JASCO V670 UV-VIS-NIR spectrophotometer in the spectral range 400 to 600 nm using a quartz cuvette with an optical path of 1 cm for samples S1, S2, and S3 at normal incidence. PL spectra of the samples were recorded with the help of LS55 Perkin Elmer Fluorescence spectrometer. FTIR spectra of the samples were recorded in the mid-infrared range at 4000–400 cm^{-1} using Bruker Alpha spectrometer. All the measurements were performed at room temperature.

RESULTS AND DISCUSSION

X-ray diffraction

X-ray diffraction is a convenient method for determining the mean size of the crystallites in nanocrystalline bulk materials by the diffracted peaks of the sample. The XRD patterns of commercially obtained and the two synthesized CdS samples are shown in **Figure 1.** which shows structural peaks diffracted by the crystal of the samples S1, S2, and S3.XRD peaks of the sample S1 are found at 26.46° (111), 43.82° (220) and 51.91° (311) which correspond to cubic phase [12] and the ones at 24.90° (100), 28.22° (002) and 47.97° (103) correspond to the hexagonal phase as reported in given references [4,7,10]. Hence, CdS sample S1 (commercially obtained) exhibits both the cubic and hexagonal phases. Peaks for sample S2 (prepared in ethanol) appearing at 26.65°, 44.23°, and 52.02° correspond to (111), (220) and (311) planes of the cubic phase [13,14]. For the sample S3 (prepared in distilled water), the peaks appear at 26.55°, 30.29°, 43.79° and 52.00° which correspond to (111), (200), (220) and (311) planes of CdS revealing the cubic crystal structure [15,16].

Research & Reviews: Journal of Material Sciences
DOI: 10.4172/2321-6212.1000167
e-ISSN: 2321-6212
p-ISSN: 2347-2278

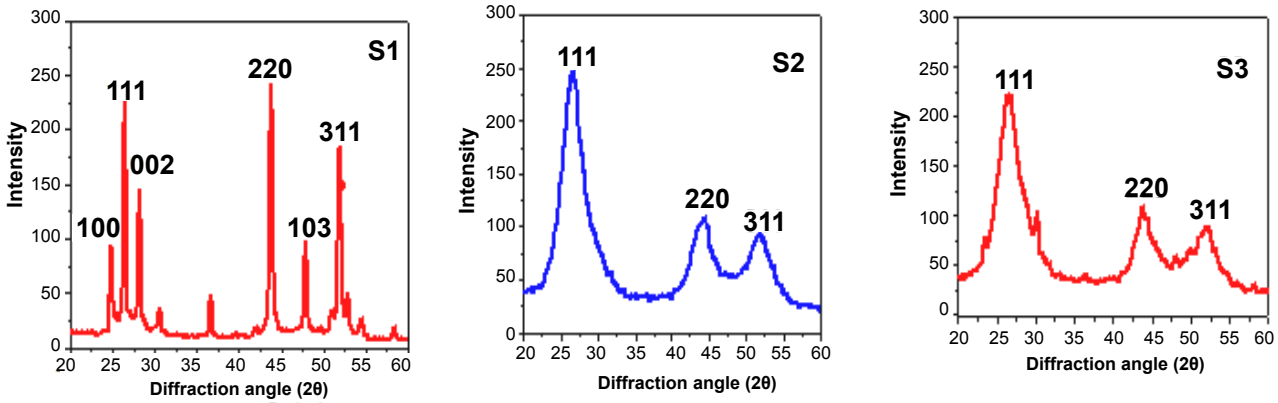

Figure 1. XRD Spectra of CdS Samples S1, S2, and S3.

The crystallite size D of the nanoparticles is calculated by Scherrer's equation $D=K\lambda/\beta\cos\theta$ where λ is the wavelength of CuK_α line, β is Full Width at Half Maximum (FWHM) of the peak or broadening of the diffraction peak and θ is the angle of diffraction [10]. The mean crystallite size of the samples S1, S2, and S3 are found to be 20.9, 3.5, and 4.9 nm respectively.

Scanning electron microscopy

In Scanning Electron Microscopy, the electrons interact with atoms in the sample, which produces various signals that can be detected. This gives important information regarding growth mechanism, shape, and size of the sample.

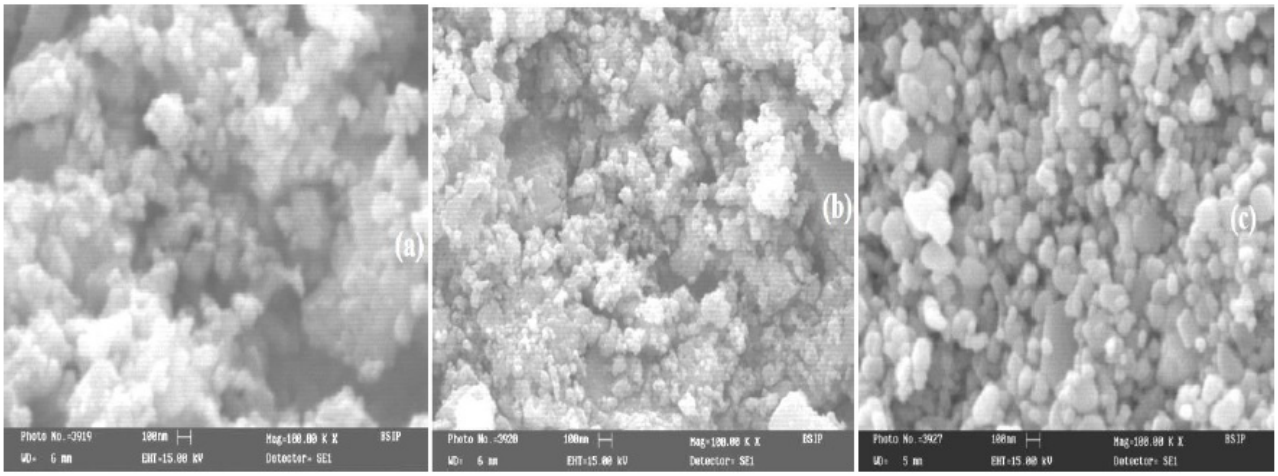

Figure 2. SEM images of CdS Samples S1 (a), S2, (b) and S3(c).

The SEM images of the CdS samples are given in Figure 2. The image of sample S1 (Figure 2a) shows spongy nature of the surface. For sample S2 (Figure 2b), the surface nature is again found to be spongy but the particles are somewhat clear. From the image of sample S3 (Figure 2c), it is observed that particles are much clear with their small clusters in 100 nm range.

OPTICAL STUDIES

UV-visible Spectroscopy

The UV-Vis absorption spectroscopy has been used to determine the size and optical properties of the quantum sized particles. When the dimensions of nanocrystalline particles approach the exciton Bohr radius, a blue shift in energy is observed due to the quantum confinement phenomena [13]. In quantum confinement effect both strong and weak confinements are possible when the particle size is less than effective Bohr radius (5.28 nm) the confinement is strong and it is weak when the Particle size is more than the Bohr radius.

The strong and weak confinement occurs due to the presence of small and large grains in the sample. In general, a nanocrystalline sample is a combination of small and large grains as the size of the particle decreases to the nanoscale the band gap of the semiconductor increases causing a blue shift in the UV-vis absorption spectra. If the absorption peaks of the prepared CdS samples appear blueshift (450-495 nm) compared with that of bulk CdS it can be easily understood that quantum confinement effect is present in the prepared CdS sample [14].

Research & Reviews: Journal of Material Sciences
DOI: 10.4172/2321-6212.1000167
e-ISSN: 2321-6212
p-ISSN: 2347-2278

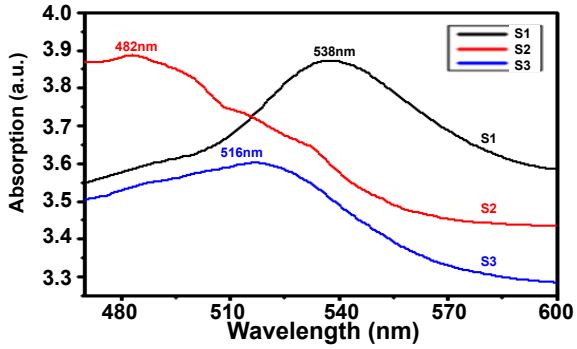

Figure 3. Absorption Spectra with wavelength of CdS Samples S1, S2, and S3.

Observed absorption spectra by UV-visible spectroscopy from the Figure 3; shows distinct spectra with a shift in wavelength, in absorption band for CdS samples are S1 (538 nm) S2 (482 nm) and S3 (516 nm) respectively. The corresponding bandgap for all the samples can be determined by using the equation $E_{np}=1240/\lambda_{max}$ is 2.30, 2.57, and 2.40 eV respectively. The spectrum of commercial CdS sample S1 exhibits a broad absorption band around 538 nm indicating the effective photoabsorption property in the visible region [15], spectra of sample S2 (prepared by ethanol) observed at 482 nm, indicates the narrow distribution of the CdS nanoparticles, it is seen that blue shift at 482 nm with respect to bulk CdS (513 nm,2.42 ev) is contributed by the quantum confinement effect [16] and absorption spectra of CdS sample S3 (prepared by distilled water) observed at 516 nm near about bulk CdS is of great interest for their practical applications such as Zero-dimensional quantum confined materials in optoelectronics and photonics [5]. Reduction in the value of measured band gap is mostly due to strongly depend on the growth condition and the reflection from defect centers in the different grown crystals of the CdS sample.

With the help of band gap value, the particle size can be calculated by Brus equation [17,18]. Since the Brus equation is used to describe the emission energy of the quantum dot semiconductor nanocrystals which gives a relation between the radius of the crystallite and the energy gap thus explains the quantum size effect. Brus et al explained the theory of the blue shift and proposed an effective mass approximation formula $E_{np}=E_o+ (h^2/8R^2)\{1/m^*_e+1/m^*_h\}$ where E_{np} is the band gap of nanoparticles, E_o is the bandgap of bulk CdS (2.42 eV), m^*_e is the effective mass of an electron (0.19 me), m^*_h is the effective mass of the hole (0.8 me) and R is the particle radius [13]. Optical size by this method for Sample S1, S2, and S3 at 2.30, 2.57, and 2.40 eV bandgap is 4.47, 4.00, and 10.96 nm respectively. The absorption spectra show a systematic blue shift, which is also confirmed by the Fluorescence measurements [19].

Absorption coefficient

Absorption coefficient (α) is the property of a material which defines the amount of incident light photon absorbed by it which depends upon incident photon energy as well as the composition of the material. Variation of absorption coefficient (α) with photon energy can be explained in term of fundamental absorption, excitation absorption and valence band acceptor absorption [20]. For many glassy and amorphous non-metallic materials, the absorption edge can be divided into three distinct regions; (i) high absorption region ($\alpha \geq 10^4$ cm^{-1}) where absorption is associated with inter-band transitions involving optical transitions between valence band and conduction band which determines the optical band gap, (ii) Spectral region with α in the range of 10^2 - 10^4 cm^{-1} is called Urbach's exponential tail region in which absorption depends exponentially on photon energy. In this region, most of the optical transitions take place between localized states and extended band states and provide information about the relative changes of the structural disorder induced by an additive [21], (iii) low absorption region ($\alpha<1$ cm^{-1}) implies weak absorption tail involving low energy absorption and originates from defects and impurities whose shape and magnitude depend on the purity, thermal history and preparation conditions [22,23].

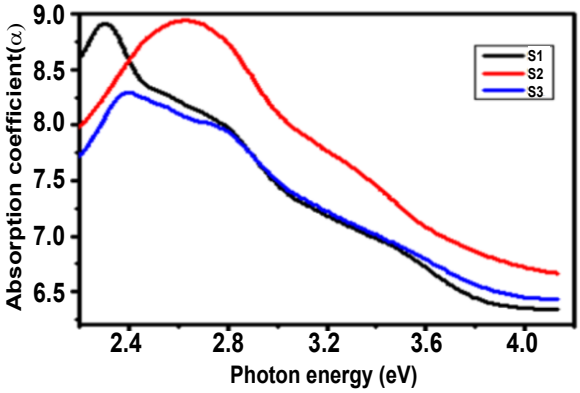

Figure 4. Absorption coefficient with photon energy for CdS Samples S1, S2, and S3.

Research & Reviews: Journal of Material Sciences
DOI: 10.4172/2321-6212.1000167
e-ISSN: 2321-6212
p-ISSN: 2347-2278

The absorption coefficient (α) has been evaluated by Beer-Lambert law (α=2.303A/t), Where A is optical absorption which depends on wavelength and density of point defects and (t) is light path length (10 mm) Figure 4 represents the absorption coefficient with incident photon energy for samples S1, S2, and S3. As the incident photon energy increases the absorption coefficient decreases continuously from visible region to near ultraviolet region. All the samples show low absorption coefficient due to defects and impurities which lead to carrier generation throughout the materials. Therefore Due to small absorption coefficient (α) of the samples S1, S2, S3, these may not be suitable for optical data storage.

Absorption constant (K)

Absorption constant/extinction coefficient indicates the amount of absorption loss when an electromagnetic wave (incident light) propagates through the material. The variation of absorption constant can be related to the variation of optical transmittance.

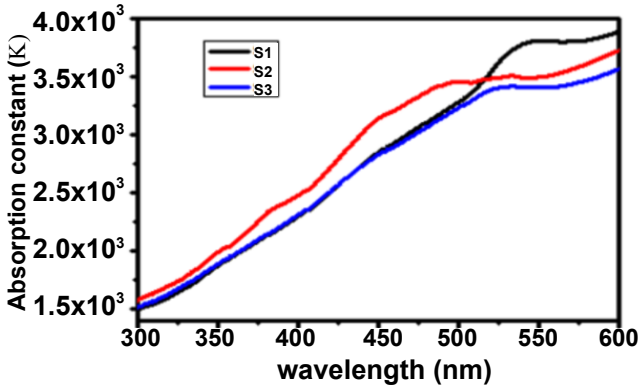

Figure 5. Absorption constant with wavelength for CdS Samples S1, S2, and S3.

Figure 5 represents the Absorption constant with increasing wavelength for samples S1, S2, and S3.As the wavelength increases the absorption constant of all the sample increases up to the visible region.Hence the maximum amount of light loss through the sample in the visible region. The absorption constant has been evaluated using formula $K=\lambda\alpha/4\pi$ [24].

Photoluminescence spectra

PL spectra provide the transition energies which can be used to determine electronic energy levels. Figure 6 shows the intensity of PL spectra with increasing wavelength of sample S1, S2, S3 at 390 nm excitation wavelength. Emission peaks have been detected at yellow band emissions at 580 nm, 584 nm and 583 nm for the samples S1, S2, and S3 respectively with highest luminous intensity for S2, S3.

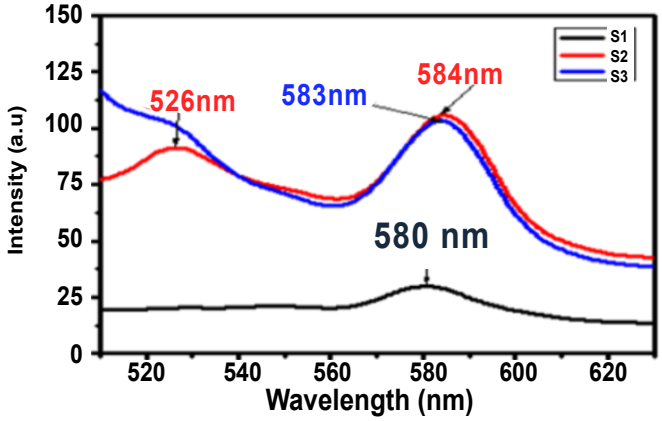

Figure 6. PL Spectra of CdS Samples S1, S2, and S3.

The green band emission observed at 526 nm for sample S2 is due to the electronic transition from conduction band to an acceptor level which is created due to the presence of interstitial sulfur ions [25]. Thus, it is seen that CdS exhibits effective photo-emission property in the visible region which shows that Lab prepared sample S2 and S3 has a minimum amount of defects in the material surface resulting increasing the PL intensity. Whereas in Sample S1 the luminous intensity decreases at lower energy are due to incomplete absorption [26].

Fourier transform infrared spectra

FTIR spectra of all three CdS samples, obtained in the mid-infrared region 4000-400 cm^{-1}, are shown in Figure 7. Each band in an infrared spectrum is assigned to a particular deformation of the molecule, the movement of a group of atoms or bending or stretching of a particular bond.

Research & Reviews: Journal of Material Sciences
DOI: 10.4172/2321-6212.1000167
e-ISSN: 2321-6212
p-ISSN: 2347-2278

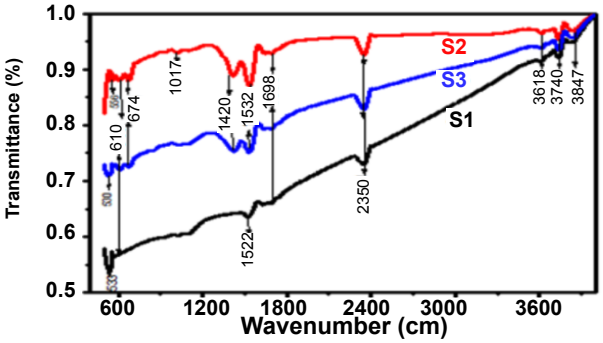

Figure 7. FTIR Spectra of CdS samples S1, S2, and S3.

The peaks observed corresponding to 1420 cm^{-1} (for samples S2 and S3), 1522 cm^{-1} (for sample S1) and 1532 cm^{-1} (for samples S2 and S3) confirm the C=O stretching of methyl group whereas the ones observed at 3618, 3740, 3847 cm^{-1} for all the three samples correspond to O-H stretching [27-29]. The peaks observed at 530 (for S2), 533 (for S1), 556 (for S2), 610 (for S2, S3), and 674 cm^{-1} (for S2, S3) represent fingerprint region of bending vibrations. Hence, peaks corresponding to 610 cm^{-1} of the samples S2 and S3 are attributed to Cd-S stretching mode of vibrations as reported by other references [19,27,29] which, besides XRD, confirm the formation of CdS.

CONCLUSION

CdS nanoparticles are synthesized by co-precipitation method. XRD pattern of the CdS samples S1 exhibits hexagonal and cubic phases while those of samples S2 and S3 show only cubic phase with average crystal size 20.9, 3.5 and 4.9 nm respectively with increasing reactivity, scattering, and surface area. From the SEM images, it is noticed that the surface morphologies are in the form of assemblies of nanoparticles. Optical size of the CdS nanoparticles by Brus equation for the samples S1, S2 and S3 are found to be 4.47, 4.00 and 10.96 nm respectively and sample S1, S2 shows a systematic blue shift which confirm the quantum confinement of the particle . The maximum absorption coefficient of all the sample observed in the visible region and continuously decreases in near ultraviolet region as photon energy increases. As the wavelength increases, absorption loss through the sample increases with decreasing transmittance in the visible region. In PL spectra yellow band observed in all three samples whereas green band observed only by sample S2.FTIR spectra, besides XRD, confirm the formation of CdS. Hence From above results, all three samples are good for optoelectronics and other application but the main focus on obtained Cadmium sulfide sample S3 (prepared in normal distilled water) gives an almost same result for optical and other characterization techniques in compare to S1, S2. It may be useful for many optoelectronic applications including solar cells, photodiodes, light emitting diodes etc. in future for general as well as scientific disciplines by easy technique and at low cost without any additional requirement.

ACKNOWLEDGEMENT

The authors express their acknowledgment to the Solid State Physics Laboratory, Delhi, India for providing facility to conduct XRD of the samples. This research did not receive any specific grant from funding agencies in the public, commercial, or not-for-profit sectors.

REFERENCES

1. Kadash E, et al. Synthesis and Characterization of Cadmium Sulfide Crystals Grown by DVT Technique. Int J Pure Appl Sci Techno 2014;22.
2. Guo A Tai, et al. Inorganic salt-induced phase control, and optical characterization of cadmium sulfide nanoparticles. Nanotechnol 2010;21.
3. Claudia Martinez-Alonso, et al. Cadmium Sulfide Nanoparticles Synthesized by Microwave Heating for Hybrid Solar Cell Applications. Int J Photo energy 2014;1-11
4. Kadam A, et al. Room temperature synthesis of CdS nanoflakes for photocatalytic properties Mater Sci: Mater Electron 2014;25:1887-1892.
5. Pendyala N, et al. Functionalized Graphite Platelets and Lead Sulfide Quantum Dots Enhance Solar Conversion Capability of a Titanium Dioxide/ Cadmium Sulfide Assembly. J Phys Chem C 2014;118: 18924-18937.
6. Brus LE. Electron-electron and electron-hole interactions in small semiconductor crystallites: The size dependence of the lowest exited electron state. J Chem Phys 1984;80:4403-4409.
7. Tessler N, et al. Efficient near-infrared polymer nanocrystals light-emitting diodes. Sci 2002;295:1506-1508.

e-ISSN: 2321-6212
p-ISSN: 2347-2278

8. Arani M and Niasari M. Synthesis, and characterization of cadmium sulfide nanocrystals in the presence of a new sulfur source via a simple solvothermal method. New J Chem 2014;38:1179-1185.

9. Qutub N and Sabir S. Optical, Thermal, and Structural Properties of CdS Quantum Dots Synthesized by A Simple Chemical Route. Int J Nanosci Nanotechnol 2012;8:111-120.

10. Mercy A, et al. Synthesis, Structural and optical characterization of cadmium sulfide nanoparticles. IJPAP 2013;51:448-452.

11. Dhage S, et al. Morphological variations in cadmium sulfide nanocrystals without phase transformation. Nanoscale Res Lett 2011;6.

12. Jadhav U, et al. Structural, optical and electrical properties of nanocrystalline cadmium sulfide thin films deposited by novel chemical route. IJPAP 2014;52:39-43.

13. Narayanan S and Pal S. Aggregated CdS Quantum Dots: Host of Bimolecular Ligands J Phys Chem B 2006;110:24403-24409.

14. ThambiDurai M, et.al. Preparation and Characterization of nanocrystalline CdS thin films. Chalcogenide Lett 2009;6:171-179.

15. Shinde KN, et al. Phosphate phosphors for Solid-state Lighting. Springer Ser Mater Sci 2013;174.

16. Murray C, et al. Synthesis and characterization of nearly monodisperse CdE (E=sulfur, selenium, tellurium) semiconductor nanocrystallites. J Am Chem Soc 1993;115:8706-8715.

17. Wang Y and Herron N. Quantum size effects on the exciton energy of CdS clusters. Phys Rev B 1990;42:7253-7255.

18. Brus L. Electronic wave functions in semiconductor clusters: experiment and theory. Phys Chem 1986;90:2555-2560.

19. Zhang WM, et al. Synthesis of Size tunable cadmium sulfide nanoparticles from a single source precursor using ammonia as the solvent. Mat. Research Bull 2011;46:2266-2270.

20. Al-Ghamdi AA. Optical band gap and optical constants in amorphous $Se_{96-X}Te_4Ag_x$ thin films. Vacuum 2006;80:400-405.

21. Halimah M, et al. Optical properties of ternary tellurite glasses. Mater Sci-Poland 2010;28:173-180.

22. Petkov P, et al. Optical Bandgap of Gallium-containing Telluride thin films'. Opt Adv Mater 2003;5:1101-1106.

23. Devika M, et al. The effect of the substrate surface on the physical properties of SnS films. Semicond Sci Technol 2006;21:1495.

24. Pandey V, et al. Optical band gap and optical constants in amorphous $Se_{70}Te_{30-x}Ag_x$ thin films. J Optoelectr Adv Mater 2006;8:789-793.

25. Kulp BA and Kelly RH. Displacement of the Sulphur Atom in CdS by Electron Bombardment. Appl Phys 1960;31.

26. Kolobov A and Tominaga J. Properties of Amorphous Chalcogenides. Springer Ser Mater Sci 2012;164.

27. Tamrakar R. Thermoluminescence studies of copper-doped cadmium sulfide nanoparticles with trap depth parameters. Res Chem Intermed 2013;39:4239-4245.

28. Duchaniya R. Optical Studies Of Chemically Synthesis CdS Nanoparticles. IJMMME 2014;2:2320-4060.

29. Giribabu K, et al. Cadmium Sulphide Nanorods; Synthesis, Characterization and their Photocatalytic Activity. Bull. Korean Chem Soc 2012;33:9.